The Cryosphere Discuss., 7, 2725–2759, 2013
www.the-cryosphere-discuss.net/7/2725/2013/
doi:10.5194/tcd-7-2725-2013

The Cryosphere Discussions
Open Access

Seasonal evolution of snow permeability under equi-temperature and temperature-gradient conditions

F. Domine[1,2], S. Morin[3], E. Brun[4], and M. Lafaysse[3]

[1]Takuvik Joint International Laboratory, Université Laval (Canada) and CNRS-INSU (France), UMI3376, Pavillon Alexandre Vachon, 1045 avenue de La Médecine, Québec, QC, G1V 0A6, Canada
[2]Department of Chemistry, Université Laval, Québec, QC, Canada
[3]Météo-France – CNRS, CNRM-GAME UMR3589, CEN, Grenoble, France
[4]Météo-France – CNRS, CNRM-GAME UMR3589, Toulouse, France

Received: 26 April 2013 – Accepted: 20 May 2013 – Published: 17 June 2013

Correspondence to: F. Domine (florent.domine@gmail.com)

Published by Copernicus Publications on behalf of the European Geosciences Union.

Abstract

The permeability K of snow to air flow affects the transfer of energy, water vapor and chemical species between the snow and the atmosphere. Yet today little is known of the temporal evolution of snow permeability as a function of metamorphic regime. Furthermore, our ability to simulate snow permeability over the seasonal evolution of a snowpack has not been tested. Here we have measured the evolution of snow permeability in a subarctic snowpack subject to high temperature-gradient (TG) metamorphism. We have also measured the evolution of the same snowpack deposited over tables so that it evolved in the equi-temperature (ET) regime. Permeability varies in the range 31×10^{-10} (ET regime) to 650×10^{-10} m^2 (TG regime). Permeability increases over time in TG conditions and decreases under ET conditions. Using measurements of density ρ and of specific surface area (SSA), from which the equivalent sphere radius r is determined, we show that the equation linking SSA, density ρ and permeability, $K = 3.0r^2e^{(-0.013\rho)}$ (with K in m^2, r in m and ρ in kg m^{-3}) obtained in a previous study adequately predicts permeability values. The detailed snowpack model Crocus is used to simulate the physical properties of the TG and ET snowpacks. For the most part, all variables are well reproduced. Simulated permeabilities are up to a factor of two greater than measurements for depth hoar layers, which we attribute to snow microstructure, as the aerodynamic properties of hollow depth hoar crystals are different from those of spheres. Finally, the large difference in permeabilities between ET and TG metamorphic regimes will impact atmosphere-snow energy and mass exchanges and these effects deserve consideration in predicting the effect of climate change on snow properties and snow-atmosphere interactions.

1 Introduction

Snow is a porous medium through which air can circulate and transfer mass and energy. Circulation can be induced over flat snow surfaces by processes such as

TCD
7, 2725–2759, 2013

turbulence (Sokratov and Sato, 2000; Clifton et al., 2008) and over rough surfaces by wind pumping (Colbeck, 1989). One noteworthy consequence of these processes is the deposition to snow of atmospheric particles such as sulphate and sea salt that affect the chemical composition of snow (Cunningham and Waddington, 1993; Domine et al., 2004; Harder et al., 1996). Examples of the importance of understanding these chemical changes include the interpretation of ice core analyses in terms of past atmospheric composition (Legrand and Mayewski, 1997) and the quantification of the sources of sea salt-derived bromine that destroys tropospheric ozone in polar regions (Simpson et al., 2005; Bottenheim et al., 2009; Spicer et al., 2002). Another consequence is that air circulation modifies the temperature and the water vapor budget of the snow in the top few cm, a process that should be accounted for for proper modeling of surface snow temperature in the presence of moderate to strong winds (Albert and Hardy, 1995; Albert and Shultz, 2002; Reimer, 1980; Sokratov and Sato, 2000).

Quantification of air flow through snow requires the knowledge of its intrinsic permeability K, as defined by Darcy's law:

$$v = -\frac{K}{\eta}\frac{\partial P}{\partial x} \tag{1}$$

where v is the air velocity, η its viscosity and $\partial P/\partial x$ is the pressure gradient along the direction of air flow. Snow permeability measurements have been done on seasonal and glacier snow (Shimizu, 1970; Albert and Perron, 2000; Albert and Shultz, 2002; Albert et al., 2000; Sommerfeld and Rocchio, 1993; Conway and Abrahamson, 1984; Arakawa et al., 2009), and the ranges of values for each snow type have been compiled by Domine et al. (2008), who show values as low as 1×10^{-10} m^2 for ice layers and as high as 800×10^{-10} m^2 for depth hoar. Given this wide range of permeability values, it appears worthwhile to be able to calculate properly this variable in snow models, as this is important for both applications mentioned above.

Equations have been proposed to relate permeability to other snow variables, and that of Shimizu (1970) which relates permeability to grain radius r and snow density ρ

TCD
7, 2725–2759, 2013

(in units of m and kg), has probably been the most widely used:

$$K = 0.308 r^2 e^{(-0.0078\rho)}, \quad (2)$$

even though it was obtained on a limited number of snow types so that its general validity has been questioned (Jordan et al., 1999). More recent work (Calonne et al., 2012; Courville et al., 2010), based on calculations from tomographic images of snow samples, offer hope of progress. Calonne et al. (2012) proposed

$$K = 3.0 r^2 e^{(-0.013\rho)}, \quad (3)$$

with K in m^2, r in m and ρ in kg m^{-3} and where equivalent sphere radius r was determined from the specific surface area (SSA) following:

$$r = 3/(\rho_{ice} SSA), \quad (4)$$

with ρ_{ice} the density of ice. Eq. (3) significantly differs from Eq. (2) for low density snows. Intuitively, the form of Eqs. (2) and (3) is easy to understand: increasing density reduces porosity and therefore pore size, thus reducing air flow. Increasing SSA (i.e. decreasing r) increases friction on surfaces, also impeding air flow.

Despite these interesting developments, little is still known about the variations of permeability during snow metamorphism. Given the relationship between K, SSA and ρ, and the fact that SSA and ρ generally decrease and increase, respectively, with time during snow metamorphism, it is not possible to predict the rate of variation of snow permeability in a given snow layer without knowing precisely the time evolution of both SSA and ρ. How K evolves with time depending on the metamorphic regime is thus an unanswered question. This work pursues three major objectives: (a) provide an independent evaluation of Eq. (3) against in-situ collocated measurements of K, SSA and ρ (Taillandier et al., 2006, 2007) (b) monitor the evolution of snow permeability of two different snowpacks, one evolving under a high temperature gradient conducive to depth hoar formation and the other one under low temperature gradient conditions

TCD
7, 2725–2759, 2013

leading mostly to the formation of small rounded grains; (c) test our ability to model the evolution of permeability using SSA and density outputs from the detailed snowpack model Crocus (Brun et al., 1992; Vionnet et al., 2012) using Eq. (3).

2 Methods

2.1 Experimental methods

The study was conducted at the Large Animal Research Station (64°52′ N–147°44′ W, 210 m a.s.l.) of the University of Alaska Fairbanks during the 2003–2004 winter, as already detailed by (Taillandier et al., 2006). The site was in a clearing and in this low wind setting the snowpack was laterally homogeneous allowing meaningful repetitive sampling of snow at several stratigraphic levels throughout the season. The climate is subarctic, with air temperature occasionally dropping below −40 °C. These low air temperatures, combined to a shallow snowpack (maximum thickness of 54 cm in late March), induce a high temperature gradient in the snowpack, which almost entirely transforms into depth hoar. This snowpack was therefore used to study permeability evolution under temperature gradient metamorphism, hereafter TG conditions following the terminology of Sommerfeld and LaChapelle (1970). In order to study evolution under low temperature gradient conditions (Equi-Temperature, or ET metamorphism after Sommerfeld and LaChapelle (1970)), the snow was allowed to deposit onto three tables 1.5 × 3 m, so that air circulation under them prevented the durable establishment of any significant temperature gradient (Taillandier et al., 2007). Alternating temperature gradients could take place in surface snow on the tables, leading to the formation of crystals having shapes similar to those produced by ET metamorphism (Pinzer and Schneebeli, 2009). However, the latitude of our site implied that the energy deposited onto the snowpack by solar radiation was very small throughout most of the winter. Temperature measurements in the snow (Taillandier et al., 2006) showed that

TCD
7, 2725–2759, 2013

significant alternating temperature gradients did not establish themselves until early March, so that the metamorphic regime was indeed essentially ET.

The tables consisted of a wooden frame over which a thin sheet of corrugated steel was screwed. A 40 µm thick polyethylene sheet was placed over the metal. This setup allows us to neglect the thermal inertia of the surface over which the table snowpack formed and to approximate the temperature at the base of the snowpack with the air temperature in calculations. The edges of the snow on the tables were protected from wind erosion by polyethylene sheets. Even though wind was never strong enough to raise snow on the ground, the table snow was more exposed and even with this precaution, a small fraction of the table snow was eroded by wind in early January, when the wind speed at 2 m reached 4.5 $m\,s^{-1}$. Other erosion episodes may have taken place but were not observed. SSA and density measurements, already reported by (Taillandier et al., 2006) started in November and ended in April. Permeability measurements were carried out on 4 February, 2 March and 25 March on the natural snowpack on the ground (hereafter: ground snowpack) and on 16 February and 9 March on the table snowpack, producing five vertical profiles of combined snow properties including SSA, density and permeability, totaling 18 snow permeability measurements (12 on ground, 6 on tables).

SSA was measured using the CH_4 adsorption method (Domine et al., 2007b). Density was measured with density cutters, using a 500 cm^3 Plexiglas tube 5 cm in inner diameter. Permeability was measured with the CRREL permeameter (Albert and Perron, 2000). Briefly, a vertical snow core 10 cm in diameter and 10 to 25 cm in height was sampled. No horizontal core could be sampled, as the weak depth hoar immediately fell apart and the structure was irremediably modified. The permeameter was installed on a table next to the sampling site, so that no sample transport was required. A pump was used to establish air flow through the snow and a differential manometer was used to measure the pressure difference between the upstream and downstream parts of the snow core. A double cylinder head minimized flow at the edge of the sample (Shimizu, 1970). A valve allowed the regulation of the flow rate, and about 10 flow

TCD
7, 2725–2759, 2013

rates were used for each sample. Plotting the pressure difference as a function of flow rate yielded a linear plot whose slope was used to determine K according to Eq. (1). Sometimes, deviations from linearity were observed at high flow rates because these were beyond the validity range of Eq. (1). Those data were discarded.

Air temperature, humidity, and wind-speed were measured on-site during the field experiment from 28 October 2003 to 22 April 2004, and are reported by Taillandier et al. (2006) and Jacobi et al. (2010).

2.2 Numerical simulations methods

The time evolution of the vertical profile of the physical properties of the snowpack was simulated using the detailed snowpack scheme Crocus (Brun et al., 1992; Vionnet et al., 2012), of the ISBA land surface model within the modeling platform SURFEX (Vionnet et al., 2012). Subsequently, we refer to the snow model as Crocus. Over the previous stand-alone version of Crocus (Brun et al., 1992; Jacobi et al., 2010), the main improvement is that the snowpack scheme is fully coupled to a soil scheme accounting for thermal diffusion (including phase-change effects) in the soil underlying the snowpack (Decharme et al., 2011). For this study, 20 soil levels were used with lower depths of 1, 3, 6, 10, 20, 30, 45, 60, 80, 100, 125, 150, 200, 250, 300, 400, 500, 650, 800 and 1000 cm below ground surface. In the case of table snowpacks, the model was modified so that air temperature was imposed to all soil layers below 10 cm, thereby mimicking the configuration on tables. The top 10 cm of soil acted to damp thermal fluctuations and prevent extensive snow melt at the base when the temperature reached 0 °C. The snowpack scheme Crocus represents the snowpack as a stack of a variable number of snow layers, depending on the total snow depth and the vertical profile of its physical properties. For this study, consistent with common practice for a seasonal snowpack (Vionnet et al., 2012), the maximum number of snow layers was 50. The model uses an internal time step of 15 min to solve the surface energy and mass balance budget, the heat diffusion equation through the snow and the soil, and the time evolution of the physical properties of snow such as density, liquid water content and microstructure

TCD
7, 2725–2759, 2013

variables (see Vionnet et al., 2012 for full details on the model). The model output consists of time series of the vertical profile of the state physical variables of the snowpack and the underlying soil, along with diagnosed quantities. In this work, emphasis is placed on the vertical profile of snow temperature, density, snow type and snow SSA. The latter two are derived from empirical variables used in Crocus to represent snow microstructure (see Morin et al., 2013 for full details). Snow permeability was computed from model-derived snow SSA and snow density according to Eq. (3) (Calonne et al., 2012).

The only deviation from the standard version of Crocus pertains to the parameterization of snow viscosity. In physically-based detailed snowpack models, snow viscosity is classically parameterized as a function of snow density and temperature (Essery et al., 2013), and generally increase with decreasing temperature to represent in a phenomenological way the impact of snow metamorphism on the rate of snow compaction. In Crocus, the temperature dependence of snow viscosity is the multiplicative factor $\exp(\alpha_\eta(T_{\mathrm{fus}} - T))$, where $\alpha_\eta = 0.1\,\mathrm{K}^{-1}$ (Vionnet et al., 2012), leading to extremely high viscosity values as soon as the snow temperature becomes lower than $-10\,^{\circ}\mathrm{C}$. To overcome unrealistic hampering of snow compaction due to sustained extremely low temperature conditions prevailing in the table snowpack (see below), this factor was bounded in the model by its value at $-7\,^{\circ}\mathrm{C}$, i.e. the maximum impact of snow temperature on snow viscosity is a factor of 2. We tested the fact that this modification has no detrimental effect on simulations carried out for snow-on-the-ground situations in environmental contexts such as alpine snowpacks and snow on the ground in Northern Eurasia using the driving and evaluation datasets described by Morin et al. (2012) and Brun et al. (2013), respectively.

To obtain a correct thermal state of the soil in our coupled soil-snow model, an eight-year spinup time was used and simulations were started on 1 July 1995. Meteorological driving data for the model consist of air temperature and humidity, wind-speed, liquid and solid precipitation rates, and shortwave and longwave downwards radiation. During spinup, we used 3 hourly data from the ERA-Interim (Dee et al., 2011) reanalysis.

TCD
7, 2725–2759, 2013

Brun et al. (2013) have shown using simulations covering Northern Eurasia that driving SURFEX/ISBA-Crocus with ERA-Interim leads to consistent simulations of the snow depth and snow water equivalent (SWE) mid-latitude low-altitude clearings. Out of an extraction grid with a spatial resolution of 0.5°, the nearest grid-point of the ERA-Interim meteorological reanalysis to the LARS was chosen, with coordinates 65° N–148° W (i.e., about 12 km from the LARS station) and a surface altitude of 341 m. The three other grid-points of the ERA-Interim analysis around the LARS site were also inspected with minimal differences in terms of meteorological forcing. Differences of meteorological fields arising from the 121 m altitude difference between the model grid-point and the experimental site were corrected using the approach described by Cosgrove et al. (2003) and used by Brun et al. (2013). The correction of the altitude difference has an insignificant impact on the meteorological forcing data and the model output. The sheltered conditions of the site made the ERA-Interim wind speed data about twice higher than in-situ data; to mitigate this discrepancy, ERA-Interim wind data were divided by 2. Starting on 29 October 2003 and until 22 April 2004, in-situ wind measurements were used.

3 Results

3.1 Description of snow conditions and snow stratigraphies on ground and tables

Data obtained on the stratigraphy, temperature gradient, density and SSA of the ground snowpack have been detailed by Taillandier et al. (2006). Additional data on this type of snowpack, and in particular details of the metamorphism of snow crystals to depth hoar, are found in Sturm and Benson (1997). Briefly, the temperature gradient in the whole snowpack decreased from a peak of 198 $K m^{-1}$ in November 2003 to a value oscillating around 20 $K m^{-1}$ in March. Most of the precipitation took place in the fall so that in early December the snowpack was already 40 cm thick. In early January, half of

TCD
7, 2725–2759, 2013

the snowpack had transformed into depth hoar, the rest being mostly faceted crystals. In late March, most of the snowpack was depth hoar, with faceted crystals near the top. The density was around 200 $kg\,m^{-3}$ throughout most of the snowpack, except near the top with values typically near 120 $kg\,m^{-3}$. The SSA of the depth hoar was in the range 6 to 14 $m^2\,kg^{-1}$, decreasing over time, while faceted crystals showed values between 9 and 17 $m^2\,kg^{-1}$. Permeability profiles are shown in Fig. 1, along with the stratigraphies. Given that cores are about 20 cm high, overlapping cores were sampled, so that what was actually measured was an average over the core.

Results from snow on tables have not been described in as much detail. Taillandier et al. (2007) briefly discussed SSA data and metamorphic conditions. More information is given here. Stratigraphies and permeability values for the table snowpack are shown in Fig. 2. The stratigraphies consists mostly of rounded or little-transformed crystals, which confirms that the table snowpack evolved essentially under ET conditions, even though thermal cycling in March did induce transient thermal gradients that produced some slight faceting. Density and SSA profiles are shown in Fig. 3, which also shows ground snowpack profiles for comparison. Snow crystal transformations were slow on the tables. Dendritic crystals had barely transformed and were still easily recognizable after several months in some thin very soft layers that were probably of very low density, but this variable could not be measured because of insufficient layer thickness. This is in agreement with the modeling study of Legagneux and Domine (2005) who showed that SSA decrease was much slower in low- than high-density snow under ET conditions. Figure 3 shows that the density profile showed a decreasing trend towards the top, as expected from compaction under ET conditions. SSA essentially decreased towards the bottom, but values never went below 12 $m^2\,kg^{-1}$, while they went below 7 $m^2\,kg^{-1}$ on the ground, because higher temperature gradients accelerate SSA decrease.

3.2 Time evolution of snow permeability

Temporal variations of permeability are shown in Fig. 4 for various levels in the snowpacks. Since cores were about 20 cm long, the levels indicate the middle of the core.

TCD
7, 2725–2759, 2013

Because core levels were not always exactly the same for all the days of the measurements, the actual level varies within a few cm. Therefore, the measurements were divided in three classes representing relative position of snow samples within the snowpack (top, middle and bottom). This allows representing the time evolution of snow permeability of approximately the same snow layers, taking into account snow compaction. Obvious trends in Fig. 4 are that K increases with time on the ground and on the contrary decreases with time on the tables.

3.3 Relationship between measured K, ρ and SSA

The present data, which combine SSA, density and permeability measurements can be used to test the relationship of Calonne et al. (2012). Figure 5 shows our data plotted together with Eq. (3) and the previous data of (Calonne et al., 2012). Other relavant data by Arakawa et al. (2009); Sommerfeld and Rocchio (1993); Courville et al. (2010) are nor reported here for clarity but can be seen in a similar graph in Calonne et al. (2012). Table 1 summarizes all the collocated measurements of permeability, SSA and density data reported in this study. The agreement is quite good, considering that our permeability measurements involve a 20 cm core, while SSA and density measurements have a resolution of 5 cm or better. This inevitably produces error and data scatter because the average permeability K of a core of height H formed of n layers of heights H_i and permeabilities K_i is given by:

$$\frac{H}{K} = \sum_{1}^{n} \frac{H_i}{K_i}, \tag{5}$$

so that thin low-permeability layers have more influence on the core permeability than thick high-permeability layers.

TCD
7, 2725–2759, 2013

3.4 Modeling results: overview of the simulations

Prior to an in-depth analysis of the numerical simulations in terms of the vertical profile of the physical properties of snow, the simulations are evaluated against measured total snow height values. Figure 6a and b shows the observed and simulated total snow height on tables and on ground, respectively. The simulations on tables show reasonable agreement between observations and simulations (bias and root mean square deviation (rmsd) of 3.8 and 8.4 cm, respectively). The model results overestimate total snow height especially starting in mid-January, when wind erosion was observed to happen on tables (but not on the ground) at the site during the experiment, which may explain the observed discrepancy. On the ground, the results of the simulations are in excellent agreement with the observations (bias and rmsd of −1.0 and 4.0 cm, respectively). Figure 6b also displays the total snow height simulated by (Jacobi et al., 2010) using the stand-alone version of Crocus. The bias and rmsd of that simulation were −1.8 and 3.9 cm, respectively, consistent with our simulations. Note, however, that to achieve such good results in terms of total snow height, (Jacobi et al., 2010) needed to manually adjust the ground flux of the stand-alone Crocus simulation. In contrast, our simulations take full advantage of the explicit coupling between the snowpack and the underlying ground, resulting in excellent agreement between model and observations without any tuning of the ground flux (Brun et al., 2013). This is best exemplified by the comparison between observed and simulated soil surface temperature (Fig. 6c).

3.5 Seasonal overview of the time evolution of physical properties of the snowpack

Figures 7 and 8 show the time evolution of the vertical profiles of several key physical snow variables: temperature, temperature gradient and main snow type, and snow density, snow SSA and snow permeability on ground and tables. The model illustrates well the contrasted thermal field within the snow between the ground and tables simulations. On ground, strong vertical gradients developed throughout the season, while on

TCD
7, 2725–2759, 2013

tables the model predicts limited temperature gradients and comparably much colder conditions (Fig. 7a–d). Since the time evolution of the grain type depends strongly on temperature and temperature gradient in Crocus (Brun et al., 1992; Vionnet et al., 2012), these results expectedly translate into widely different predicted snow types, as shown on Fig. 7e, f. Snow on tables is simulated to evolve slowly into rounded grains, then faceted crystals, while snow on the ground evolves much quicker into mostly depth hoar. Grain type simulations are mostly consistent with observations. However, the transformation of basal melt forms into depth hoar on the ground, visible in Fig. 1 and detailed in (Domine et al., 2009), is not simulated here. Likewise, the preservation of dendritic crystals until the end of the season (Fig. 2) is not reproduced, but the layers involved are very thin, so that the layer treatment in Crocus does not allow the conservation of these limited amounts of precipitation as individual layers (Vionnet et al., 2012).

The time evolution of the physical properties of all the snow layers making up the snowpack (density, SSA and permeability) is displayed on Fig. 9. To produce such plots, individual layers were identified using the date of snowfall which is a tracer within the snowpack model, and the average and standard deviation of the relevant physical quantity for all snow layers as a function of their age was computed. The density increases in both cases at a comparable rate, and SSA exhibits a faster decrease on the ground (larger temperature and temperature gradient) than on tables, consistent with the present field experiment and previous investigations (Taillandier et al., 2007; Flanner and Zender, 2006). The time evolution of snow permeability shows contrasted time evolutions. On tables, K initially increases from values on the order of 30 to 60 10^{-10} m^2 in fresh snow to reach a maximum value around 200 10^{-10} m^2 after ca. 20 days and then starts to decrease. On ground on the contrary values keep increasing up to about 1000 10^{-10} m^2 after 60 to 70 days, where permeability values tend to stabilize or perhaps show an insignificant decrease. Here again, the model results follows qualitatively the experimental data reported in Fig. 4.

TCD
7, 2725–2759, 2013

3.6 Comparison of vertical profiles

Quantitative comparisons between observations and simulations of snow density, SSA and permeability were carried out, and we present here the data for those profiles for which all three variables were measured. Figures 10 and 11 show the measured and simulated profiles of the three variables on ground (3 profiles) and on tables (2 profiles). They illustrate in greater detail than previously the agreement and discrepancy between observed and simulated physical properties of snow. To quantitatively compare observed and simulated data, the high-resolution simulated profiles were integrated over the measurement height. In the case of SSA and density, the weighting was carried out as a function of the layer thickness. In the case of permeability, Eq. (5) was used. Table 2 summarizes the model/measurements rmsd and bias for these three variables.

On the ground, the main discrepancies are the strong overestimation of snow density in the lowermost part of the snowpack, up to 100 $\mathrm{kg\,m^{-3}}$. This discrepancy decreases towards the end of the season. On tables, the main discrepancies lie in the upper part of the profile, due to the overestimation of total snow height by the model. The main cause of this overestimation is wind erosion, which was observed at the site but not accounted for in the model simulations. In terms of snow SSA, the agreement between the model and the observations is very satisfying, with negligible bias on tables and on the ground. The striking difference between the observed and simulated profiles of snow permeability is the existence of several layers with a high permeability in the middle of the ground snowpack, featuring permeability values above 1000 $10^{-10}\,\mathrm{m^2}$. None of the measurements display such high values, which is only in part due to the averaging procedure: vertically integrated values are generally higher than the corresponding observed data, within up to a factor 2 difference. The average bias between model results and measurement is on the order of 40 % with a rmsd of 40 %, which is satisfactory given the large scatter in existing field measurements of permeability (Calonne et al., 2012) and the many possible sources of error of the simulated data.

TCD
7, 2725–2759, 2013

4 Discussion

4.1 Comparison between measurements and model

Despite the generally good agreement between measurement and model seen in Figs. 6, 10 and 11, some differences require discussion. The first one is the density profiles of the ground snowpack. While measurements show a fairly flat profiles with densities in the lower two thirds essentially constant around 200 $kg\,m^{-3}$, simulations show a profile that decreases with height. In addition to the impact of a rain-on-snow event in the beginning of the season, which shows more clearly on the simulations than on the field observations, we believe that this is because Crocus does not currently take into account the upward water vapor flux induced by the large temperature gradient. Sturm and Benson (1997) showed with water isotopes measurements that these fluxes indeed led to extensive mass redistribution.

The largest difference is between measured and simulated permeabilities, and the difference reaches a factor of two for some of the depth hoar samples. We propose that this may be explained by the peculiar shapes of depth hoar crystals. Permeability estimates are based on density and SSA according to Eq. (4). Taillandier et al. (2007) showed (their Fig. 1) that depth hoar crystals, which are hollow, have a much larger visible size that predicted by Eq. (3). Following Taillandier et al. (2007), a depth hoar crystal with SSA = 16.4 $m^2\,kg^{-1}$ has an equivalent sphere diameter of 0.4 mm, but its visible size is > 2 mm. Its aerodynamic drag will therefore be much larger than that of the small sphere, leading to a lower permeability that predicted by spheres of the same SSA. Furthermore, our measurement method had air flowing from bottom to top. Since depth hoar crystals are shaped as hollow cups with their opening facing down (Sturm and Benson, 1997), this configuration will maximize drag, also reducing air flow and decreasing permeability. In summary, we suggest that the difference between measurement and model are caused by microstructure, which the permeability parameterization does not account for. This stresses the need for further studies addressing the complex relationships between permeability and microstructure (not only

TCD
7, 2725–2759, 2013

density and SSA) in parallel to model developments aimed at simulating the relevant microstructure variables needed for such improved parameterizations.

4.2 Metamorphism, climate and permeability

This study constitutes a novel illustration of the difference between ET and TG metamorphism, already well documented with regards to crystal morphology and density (e.g. Colbeck, 1983; Sommerfeld and LaChapelle, 1970; and to SSA Taillandier et al., 2007). Here we show that these different regimes manifest themselves very clearly in permeability values and in the time-evolution of permeability. In the ET regime, compaction reduces porosity, contributing to permeability decrease over time. Figure 4 shows that this decrease is not compensated by the decrease in SSA, which should lead to a permeability increase, as indicated by Eq. (3). In the intense TG conditions of the ground snowpack, the formation of large grains and the lack of compaction beyond densities of about 200 $\mathrm{kg\,m^{-3}}$, coupled to a rapid SSA decrease, result in the formation of large pores that facilitate air flow, so that values exceed $500 \times 10^{-10}\ \mathrm{m^2}$ in the bottom half of the snowpack at the end of the season. We note however that we measured vertical permeability, while air advection will also be sensitive to horizontal permeability. Calonne et al. (2012) have calculated that anisotropy might reach a factor of 1.6 for depth hoar, so that horizontal permeability could be somewhat lower than what we measured. Further delicate measurements are required to confirm these calculations. Still, at the end of the season, permeability in TG snow is much greater than in ET snow, by a factor of 10 for vertical permeability.

This indicates that changes in snow properties due to climate change (Domine et al., 2007a) will affect both energy transfer due to air advection and the deposition of chemicals to snow by the filtering of advected air. These effects should be taken into account when quantifying snow-climate feedbacks. Detailing them is beyond our scope but a couple of examples may be mentioned. First the warming of the boreal forest will limit depth hoar development and therefore reduce both above effects. Second, changes in the properties of tundra snowpacks (Domine et al., 2012) are more complex. The

TCD
7, 2725–2759, 2013

warming-induced growth of vegetation will change snow properties by sheltering snow from wind effects and limiting the formation of low-permeability Arctic wind slabs on the surface (Gouttevin et al., 2012). Depth hoar development will be more likely, and this will increase the potential for air advection. However, this will also probably reduce surface roughness, so that wind pumping will be less efficient (Colbeck, 1989; Cunningham and Waddington, 1993). The impact of rain-on-snow events also needs to be included in such a discussion, which is beyond the scope of the current study. Determining the resulting effect on energy and chemical transfer in the top layers of the snowpacks will require further work that takes into account changes in wind speed, snow permeability and surface roughness.

5 Conclusions

Regarding the main three objectives of this study, we conclude that the metamorphic regime of the snow has a very strong effect on snow permeability and on its evolution. The TG regime leads to high values increasing over time, while the ET regime features low values decreasing over time. Then, as shown in Fig. 5, Eq. (3) is verified by our measurements, despite the fact that we used vertical cores about 20 cm high, where low permeability layers have an important effect. This equation, when applied together with outputs of the snowpack model Crocus, allows the reasonable simulation of snow permeability. Differences of up to a factor of two observed for depth hoar suggest that grain shape and snow microstructure should be taken into account for improved accuracy in simulating snow permeability.

Acknowledgements. The experimental part of this work was partially supported by Chapman Chair funds, kindly supplied by the late Norbert Untersteiner during F. D.'s stay at the Geophysical Institute, University of Alaska Fairbanks. F. D. is very indebted to William R. Simpson for organizing his stay at UAF, and thanks Matthew Sturm for the use of the permeameter, as well as Anne-Sophie Taillandier for assistance with some of the measurements. Bill Hauer very kindly proposed the LARS site for the experimental part of this study and provided assistance

TCD
7, 2725–2759, 2013

throughout the field work. We are grateful to J.-M. Willemet (CNRM-GAME/CEN), the SURFEX support team (CNRM-GAME) for their help in maintaining and using the model and F. Flin and N. Calonne (CNRM-GAME/CEN) for discussions related to snow permeability estimates from snow microstructure variables.

The publication of this article is financed by CNRS-INSU.

References

Albert, M. R. and Hardy, J. P.: Ventilation experiments in a seasonal snow cover, in: Biogeochemistry of Seasonally Snow-Covered Catchments, IAHS Publications, Boulder, CO, 1995, 41–49, 1995.

Albert, M. R. and Perron, F. E.: Ice layer and surface crust permeability in a seasonal snow pack, Hydrol. Processes, 14, 3207–3214, 2000.

Albert, M. R. and Shultz, E. F.: Snow and firn properties and air-snow transport processes at Summit, Greenland, Atmos. Environ., 36, 2789–2797, 2002.

Albert, M. R., Shultz, E. F., and Perron, F. E.: Snow and firn permeability at Siple Dome, Antarctica, Ann. Glaciol., 31, 353–356, 2000.

Arakawa, H., Izumi, K., Kawashima, K., and Kawamura, T.: Study on quantitative classification of seasonal snow using specific surface area and intrinsic permeability, Cold Regions Sci. Tech., 59, 163–168, 2009.

Bottenheim, J. W., Netcheva, S., Morin, S., and Nghiem, S. V.: Ozone in the boundary layer air over the Arctic Ocean: measurements during the TARA transpolar drift 2006–2008, Atmos. Chem. Phys., 9, 4545–4557, doi:10.5194/acp-9-4545-2009, 2009.

Brun, E., David, P., Sudul, M., and Brunot, G.: A numerical-model to simulate snow-cover stratigraphy for operational avalanche forecasting, J. Glaciol., 38, 13–22, 1992.

Brun, E., Vionnet, V., Boone, A., Decharme, B., Peings, Y., Valette, R., Karbou, F., and Morin, S.: Simulation of northern Eurasian local snow depth, mass and density using a de-

TCD

7, 2725–2759, 2013

tailed snowpack model and meteorological reanalysis, J. Hydrometeorol., 14, 203–214, doi:10.1175/jhm-d-12-012.1, 2013.
Calonne, N., Geindreau, C., Flin, F., Morin, S., Lesaffre, B., Rolland du Roscoat, S., and Charrier, P.: 3-D image-based numerical computations of snow permeability: links to specific surface area, density, and microstructural anisotropy, The Cryosphere, 6, 939–951, doi:10.5194/tc-6-939-2012, 2012.
Clifton, A., Manes, C., Ruedi, J. D., Guala, M., and Lehning, M.: On shear-driven ventilation of snow, Bound.-Layer Meteorol., 126, 249–261, doi:10.1007/s10546-007-9235-0, 2008.
Colbeck, S. C.: Theory of metamorphism of dry snow, J. Geophys. Res., 88, 5475–5482, 1983.
Colbeck, S. C.: Air movement in snow due to windpumping, J. Glaciol., 35, 209–213, 1989.
Conway, H. and Abrahamson, J.: Air permeability as a textural indicator of snow, J. Glaciol., 30, 328–333, 1984.
Cosgrove, B. A., Lohmann, D., Mitchell, K. E., Houser, P. R., Wood, E. F., Schaake, J. C., Robock, A., Sheffield, J., Duan, Q. Y., Luo, L. F., Higgins, R. W., Pinker, R. T., and Tarpley, J. D.: Land surface model spin-up behavior in the North American Land Data Assimilation System (NLDAS), J. Geophys. Res., 108, D8845, doi:10.1029/2002jd003316, 2003.
Courville, Z., Hoerhold, M., Hopkins, M., and Albert, M.: Lattice-Boltzmann modeling of the air permeability of polar firn, J. Geophys. Res., 115, F04032 doi:10.1029/2009jf001549, 2010.
Cunningham, J. and Waddington, E. D.: Air-flow and dry deposition of non-sea salt sulfate in polar firn – Paleoclimatic implications, Atmos. Environ. A, 27, 2943–2956, doi:10.1016/0960-1686(93)90327-u, 1993.
Decharme, B., Boone, A., Delire, C., and Noilhan, J.: Local evaluation of the Interaction between Soil Biosphere Atmosphere soil multilayer diffusion scheme using four pedotransfer functions, J. Geophys. Res., 116, D20126, doi:10.1029/2011jd016002, 2011.
Dee, D. P., Uppala, S. M., Simmons, A. J., Berrisford, P., Poli, P., Kobayashi, S., Andrae, U., Balmaseda, M. A., Balsamo, G., Bauer, P., Bechtold, P., Beljaars, A. C. M., van de Berg, L., Bidlot, J., Bormann, N., Delsol, C., Dragani, R., Fuentes, M., Geer, A. J., Haimberger, L., Healy, S. B., Hersbach, H., Holm, E. V., Isaksen, L., Kallberg, P., Kohler, M., Matricardi, M., McNally, A. P., Monge-Sanz, B. M., Morcrette, J. J., Park, B. K., Peubey, C., de Rosnay, P., Tavolato, C., Thepaut, J. N., and Vitart, F.: The ERA-Interim reanalysis: configuration and performance of the data assimilation system, Q. J. Roy. Meteorol. Soc., 137, 553–597, doi:10.1002/qj.828, 2011.

TCD
7, 2725–2759, 2013

Domine, F., Sparapani, R., Ianniello, A., and Beine, H. J.: The origin of sea salt in snow on Arctic sea ice and in coastal regions, Atmos. Chem. Phys., 4, 2259–2271, doi:10.5194/acp-4-2259-2004, 2004.

Domine, F., Taillandier, A. S., Houdier, S., Parrenin, F., Simpson, W. R., and Douglas, T. A.: Interactions between snow metamorphism and climate: physical and chemical aspects, in: Physics and Chemistry of Ice, edited by: Kuhs, W. F., Royal Society of Chemistry, UK, Cambridge, 27–46, 2007a.

Domine, F., Taillandier, A. S., and Simpson, W. R.: A parameterization of the specific surface area of seasonal snow for field use and for models of snowpack evolution, J. Geophys. Res., 112, F02031, doi:10.1029/2006jf000512, 2007b.

Domine, F., Albert, M., Huthwelker, T., Jacobi, H.-W., Kokhanovsky, A. A., Lehning, M., Picard, G., and Simpson, W. R.: Snow physics as relevant to snow photochemistry, Atmos. Chem. Phys., 8, 171–208, doi:10.5194/acp-8-171-2008, 2008.

Domine, F., Taillandier, A.-S., Cabanes, A., Douglas, T. A., and Sturm, M.: Three examples where the specific surface area of snow increased over time, The Cryosphere, 3, 31–39, doi:10.5194/tc-3-31-2009, 2009.

Domine, F., Gallet, J.-C., Bock, J., and Morin, S.: Structure, specific surface area and thermal conductivity of the snowpack around Barrow, Alaska, J. Geophys. Res., 117, D00R14, doi:10.1029/2011jd016647, 2012.

Essery, R., Morin, S., Lejeune, Y., and Ménard, C. B.: A comparison of 1701 snow models using observations from an alpine site, Adv. Water Resour., 55, 131–148, doi:10.1016/j.advwatres.2012.07.013, 2013.

Fierz, C., Armstrong, R. L., Durand, Y., Etchevers, P., Greene, E., McClung, D. M., Nishimura, K., Satyawali, P. K., and Sokratov, S. A.: The International classification for seasonal snow on the ground UNESCO-IHP, ParisIACS Contribution N°1, 80, 2009.

Flanner, M. G. and Zender, C. S.: Linking snowpack microphysics and albedo evolution, J. Geophys. Res., 111, D12208, doi:10.1029/2005jd006834, 2006.

Gouttevin, I., Menegoz, M., Dominé, F., Krinner, G., Koven, C., Ciais, P., Tarnocai, C., and Boike, J.: How the insulating properties of snow affect soil carbon distribution in the continental pan-Arctic area, J. Geophys. Res., 117, G02020, doi:10.1029/2011jg001916, 2012.

Harder, S. L., Warren, S. G., Charlson, R. J., and Covert, D. S.: Filtering of air through snow as a mechanism for aerosol deposition to the Antarctic ice sheet, J. Geophys. Res., 101, 18729–18743, doi:10.1029/96jd01174, 1996.

TCD
7, 2725–2759, 2013

Jacobi, H. W., Domine, F., Simpson, W. R., Douglas, T. A., and Sturm, M.: Simulation of the specific surface area of snow using a one-dimensional physical snowpack model: implementation and evaluation for subarctic snow in Alaska, The Cryosphere, 4, 35–51, doi:10.5194/tc-4-35-2010, 2010.

Jordan, R. E., Hardy, J. P., Perron, F. E., and Fisk, D. J.: Air permeability and capillary rise as measures of the pore structure of snow: an experimental and theoretical study, Hydrol. Processes, 13, 1733–1753, doi:10.1002/(SICI)1099-1085(199909)13:12/13<1733::AID-HYP863>3.0.CO;2-2, 1999.

Legagneux, L. and Domine, F.: A mean field model of the decrease of the specific surface area of dry snow during isothermal metamorphism, J. Geophys. Res., 110, F04011, doi:10.1029/2004jf000181, 2005.

Legrand, M. and Mayewski, P.: Glaciochemistry of polar ice cores: a review, Rev. Geophys., 35, 219–243, doi:10.1029/96rg03527, 1997.

Morin, S., Lejeune, Y., Lesaffre, B., Panel, J.-M., Poncet, D., David, P., and Sudul, M.: An 18-yr long (1993–2011) snow and meteorological dataset from a mid-altitude mountain site (Col de Porte, France, 1325 m alt.) for driving and evaluating snowpack models, Earth Syst. Sci. Data, 4, 13–21, doi:10.5194/essd-4-13-2012, 2012.

Morin, S., Domine, F., Dufour, A., Lejeune, Y., Lesaffre, B., Willemet, J. M., Carmagnola, C. M., and Jacobi, H. W.: Measurements and modeling of the vertical profile of specific surface area of an alpine snowpack, Adv. Water Resour., 55, 111–120, doi:10.1016/j.advwatres.2012.01.010, 2013.

Pinzer, B. R. and Schneebeli, M.: Snow metamorphism under alternating temperature gradients: morphology and recrystallization in surface snow, Geophys. Res. Lett., 36, L23503, doi:10.1029/2009gl039618, 2009.

Reimer, A.: The effect of wind on heat transfer in snow, Cold Regions Sci. Tech., 3, 129–137, doi:10.1016/0165-232x(80)90017-8, 1980.

Shimizu, H.: Air permeability of deposited snow, Low Temp. Sci. Contrib. Ser. A, 22, 29–35, 1970.

Simpson, W. R., Alvarez-Aviles, L., Douglas, T. A., Sturm, M., and Domine, F.: Halogens in the coastal snow pack near Barrow, Alaska: evidence for active bromine air-snow chemistry during springtime, Geophys. Res. Lett., 32, L04811, doi:10.1029/2004gl021748, 2005.

Sokratov, S. A. and Sato, A.: Wind propagation to snow observed in laboratory, edited by: Steffen, K., Ann. Glaciol., 31, 427–433, 2000.

TCD
7, 2725–2759, 2013

Sommerfeld, R. A. and LaChapelle, E.: The classification of snow metamorphism, J. Glaciol., 9, 3–17, 1970.
Sommerfeld, R. A. and Rocchio, J. E.: Permeability measurements on new and equitemperature snow, Water Resour. Res., 29, 2485–2490, 1993.
Spicer, C. W., Plastridge, R. A., Foster, K. L., Finlayson-Pitts, B. J., Bottenheim, J. W., Grannas, A. M., and Shepson, P. B.: Molecular halogens before and during ozone depletion events in the Arctic at polar sunrise: concentrations and sources, Atmos. Environ., 36, 2721–2731, 2002.
Sturm, M. and Benson, C. S.: Vapor transport, grain growth and depth-hoar development in the subarctic snow, J. Glaciol., 43, 42–59, 1997.
Taillandier, A. S., Domine, F., Simpson, W. R., Sturm, M., Douglas, T. A., and Severin, K.: Evolution of the snow area index of the subarctic snowpack in central Alaska over a whole season. Consequences for the air to snow transfer of pollutants, Environ. Sci. Technol., 40, 7521–7527, doi:10.1021/es060842j, 2006.
Taillandier, A. S., Domine, F., Simpson, W. R., Sturm, M., and Douglas, T. A.: Rate of decrease of the specific surface area of dry snow: isothermal and temperature gradient conditions, J. Geophys. Res., 112, F03003, doi:10.1029/2006jf000514, 2007.
Vionnet, V., Brun, E., Morin, S., Boone, A., Faroux, S., Le Moigne, P., Martin, E., and Willemet, J.-M.: The detailed snowpack scheme Crocus and its implementation in SURFEX v7.2, Geosci. Model Dev., 5, 773–791, doi:10.5194/gmd-5-773-2012, 2012.

TCD
7, 2725–2759, 2013

Table 1. Overview of combined snow permeability, density and SSA data acquired in the field during the experiment.

Date	Location	Height min	Height max	Density	SSA	Permeability	Snow type
		cm	cm	kg m^{-3}	m^2 kg^{-1}	10^{-10} m^2	ICSSG
12 Feb 2004	Ground	37	47	120	18	97	DF(FC)
12 Feb 2004	Ground	19	36	175	11	222	FC
12 Feb 2004	Ground	6	23	201	8	476	DH
12 Feb 2004	Ground	4	20	210	7	346	DH
12 Feb 2004	Ground	0	17	205	7	374	DH
16 Feb 2004	Table	21	40	135	20	68	DF(RG)
16 Feb 2004	Table	1	21	220	14	43	RG(DF)
2 Mar 2004	Ground	26	48	145	15	159	FC(DH)
2 Mar 2004	Ground	22	44	160	12	128	FC(DH)
2 Mar 2004	Ground	9	31	200	8	398	DH
2 Mar 2004	Ground	0	22	200	7	400	DH
9 Mar 2004	Table	15	36	160	16	52	DF(RG)
9 Mar 2004	Table	7	29	230	14	42	RG(FC)
9 Mar 2004	Table	4	25	230	12	40	RG(FC)
9 Mar 2004	Table	2	23	240	13	31	RG(FC)
25 Mar 2004	Ground	27	48	160	11	219	FC(DH)
25 Mar 2004	Ground	16	36	200	7	648	DH(FC)
25 Mar 2004	Ground	0	22	220	6	522	DH

TCD
7, 2725–2759, 2013

Table 2. Statistical summary of relative differences between simulated and observed properties of the snowpack (density, SSA and permeability).

Variable	Location	n	Bias	RMSD
Density (kg m^{-3})	Ground	34	13.4	38.2
	Tables	17	22.1	28.7
	All	51	16.3	35.3
SSA (m^2 kg^{-1})	Ground	15	−1.6	3.5
	Tables	12	−3.9	7.5
	All	27	−2.6	5.7
Permeability (10^{-10} m^2)	Ground	11	198.1	321.3
	Table	6	20.6	22.1
	All	17	135.5	258.8

TCD
7, 2725–2759, 2013

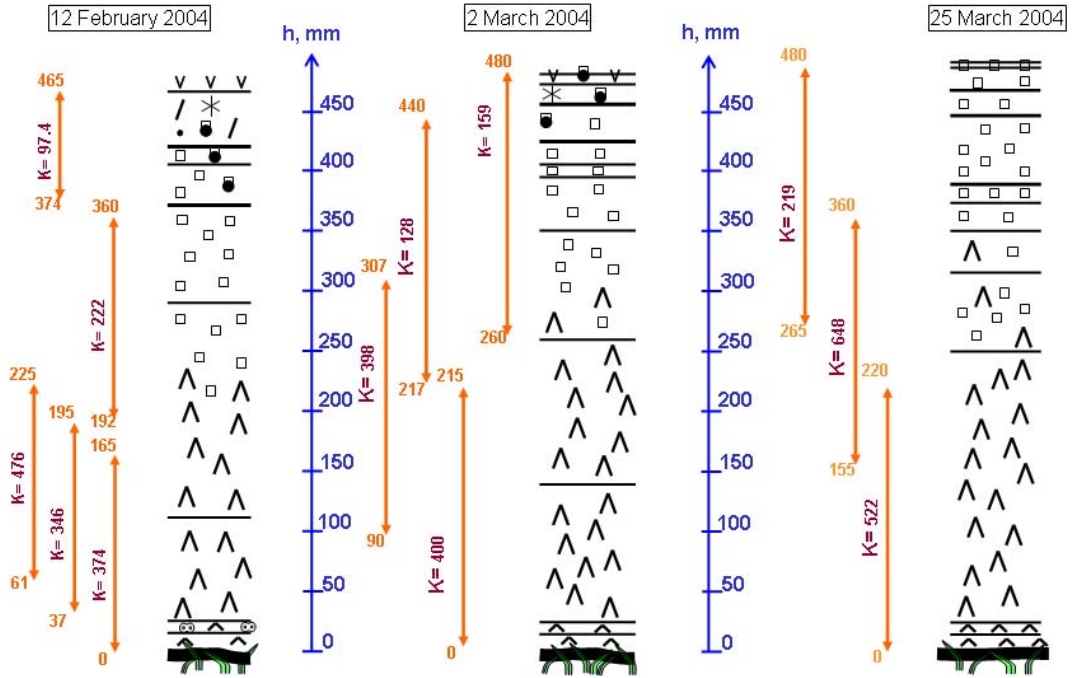

Fig. 1. Stratigraphy and permeability K, in units of $10^{-10}\,m^2$, of snow cores sampled at the levels indicated by the orange arrows, for the ground snowpack. Snow cores were about 20 cm tall, and the heights of their bases and tops are shown (in mm for better precision) at each end of the orange arrows. Symbols are from the International Classification of Seasonal Snow on the Ground (Fierz et al., 2009).

TCD
7, 2725–2759, 2013

Seasonal evolution of snow permeability under ET and TG conditions

F. Domine et al.

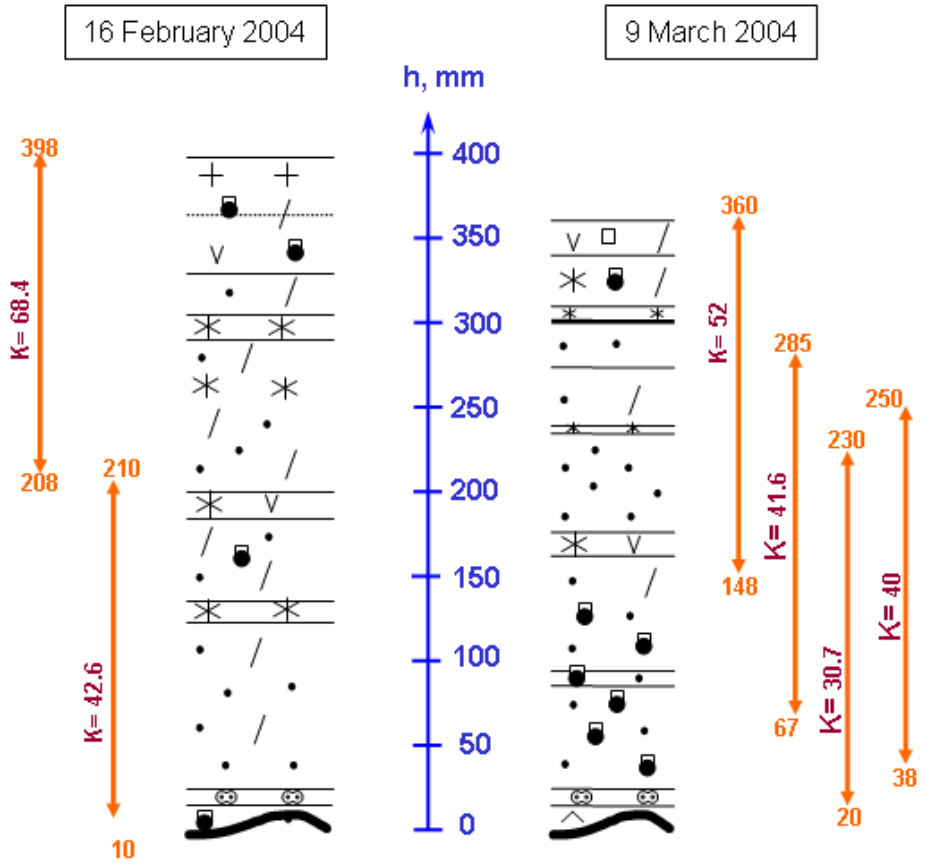

Fig. 2. Same as Fig. 1, for the table snowpack.

TCD
7, 2725–2759, 2013

Seasonal evolution of snow permeability under ET and TG conditions

F. Domine et al.

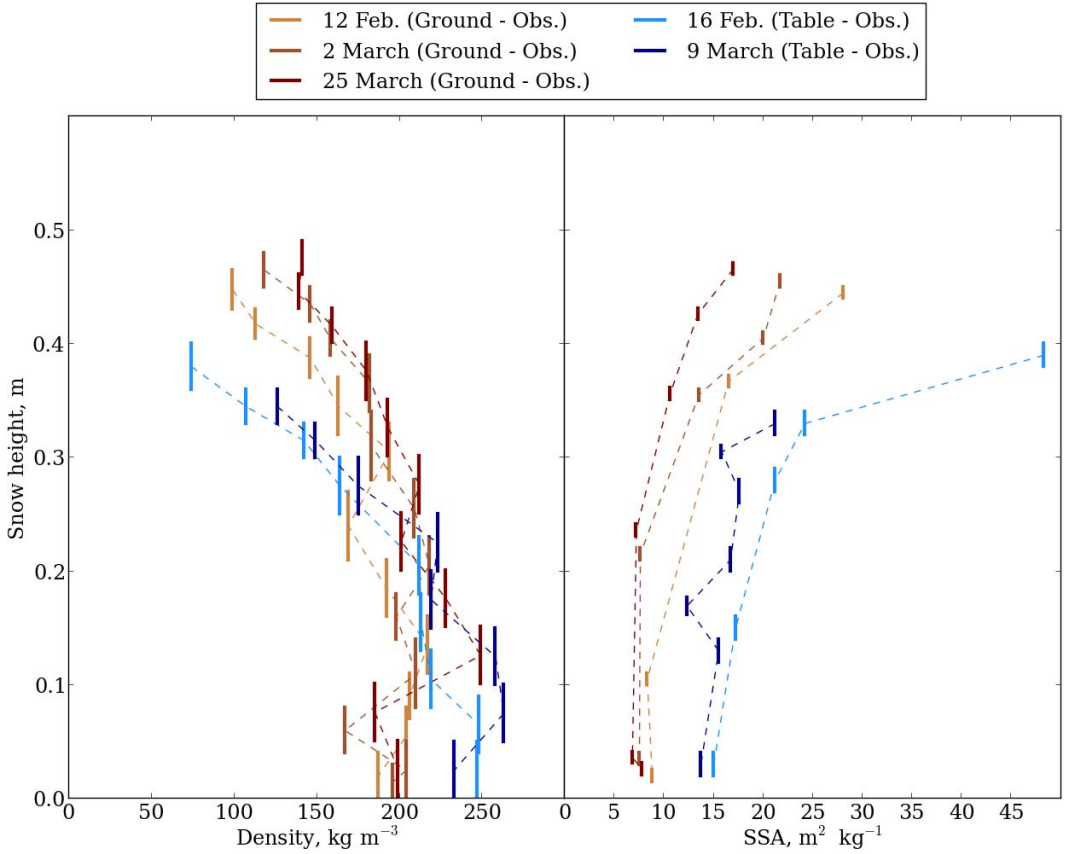

Fig. 3. Vertical profiles of density and specific surface area (SSA) for the ground and table snowpacks. The height of the vertical bars shows the range of snow heights that were actually sampled. The dotted lines joining the data bars are visual aids.

TCD
7, 2725–2759, 2013

Seasonal evolution of snow permeability under ET and TG conditions

F. Domine et al.

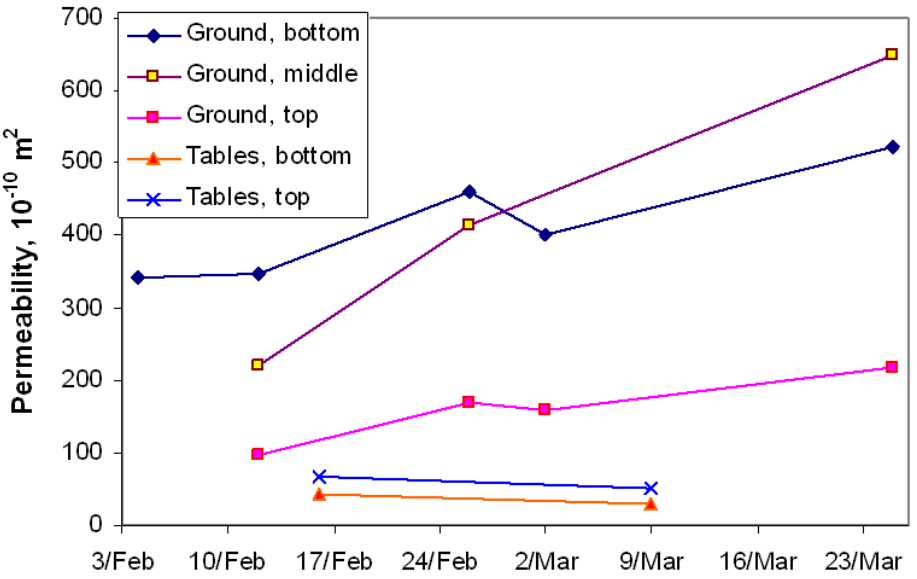

Fig. 4. Time-evolution of snow permeability on the table and ground, for different regions of the snowpack. Heights where measurements were made are not exactly constant, due to variations in the location of the cores and to compaction of the layers that were followed. Average heights of the center of the cores used were (above ground) 11, 26 and 39 cm for the bottom, middle and top cores on the ground, and 12 and 27 cm for the bottom and top cores on the tables, respectively. Isolated data points obtained on 4 and 26 February, not shown in Fig. 1, have been reported here.

TCD
7, 2725–2759, 2013

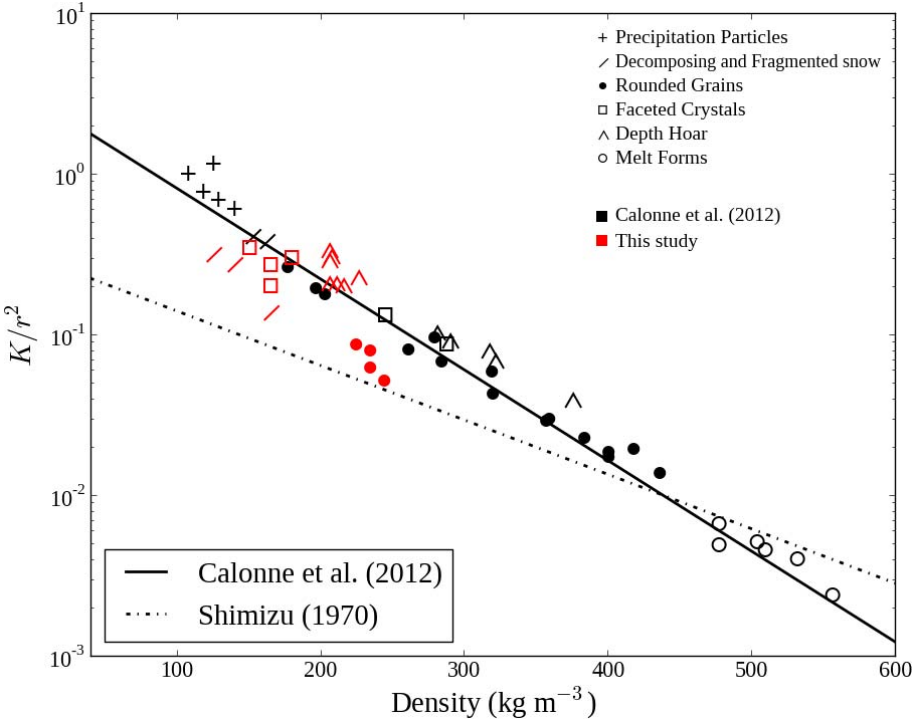

Fig. 5. Comparison of our experimental data (in red) with Eq. (3). The widely used equation of Shimizu (1970) is also plotted. Data from Calonne et al. (2012) are also shown.

TCD
7, 2725–2759, 2013

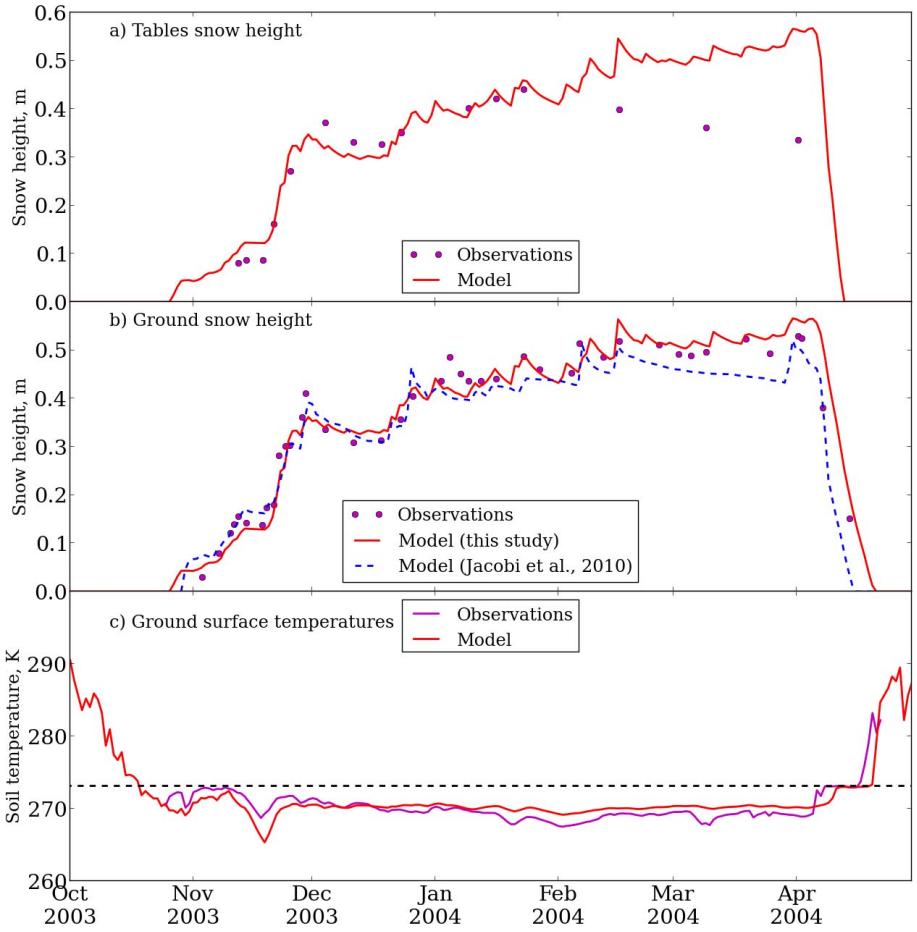

Fig. 6. Simulations of the seasonal evolution of snowpack height with Crocus. **(a)** On tables; **(b)** on the ground. Experimental data and the previous work of Jacobi et al. (2010) are also shown for comparison. Panel **(c)** displays the simulated and observed ground surface temperature.

TCD
7, 2725–2759, 2013

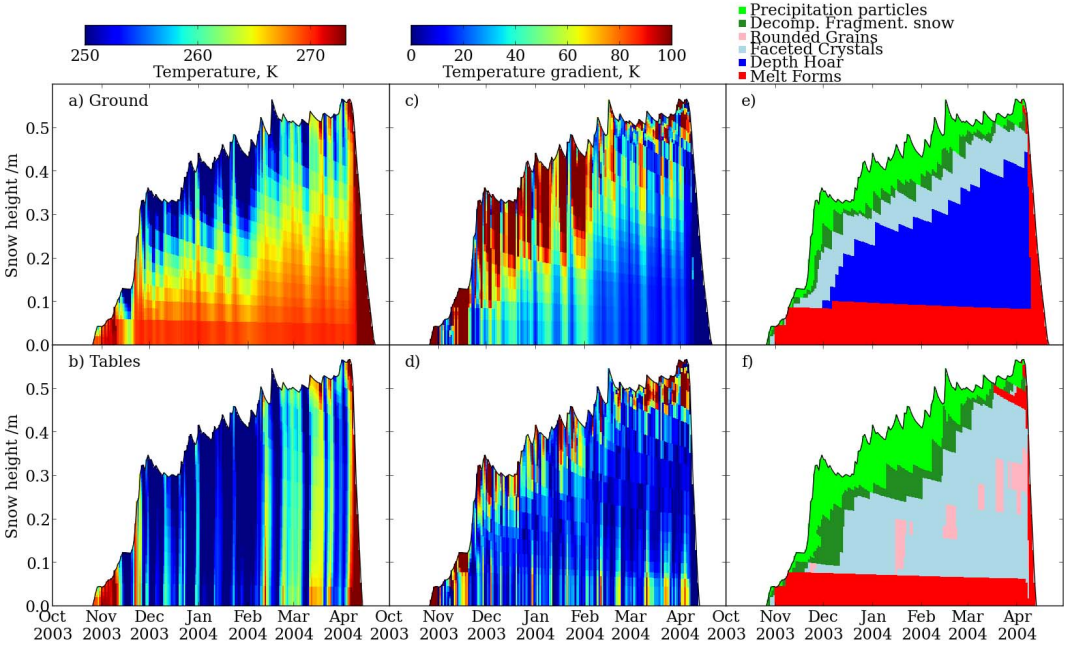

Fig. 7. Simulations of the vertical profiles of temperature (**a** and **b**), temperature gradient (**c** and **d**) and crystal type (**e** and **f**) on the ground **(a, c, d)** and on tables **(b, d, f)** using Crocus, over the whole season.

TCD
7, 2725–2759, 2013

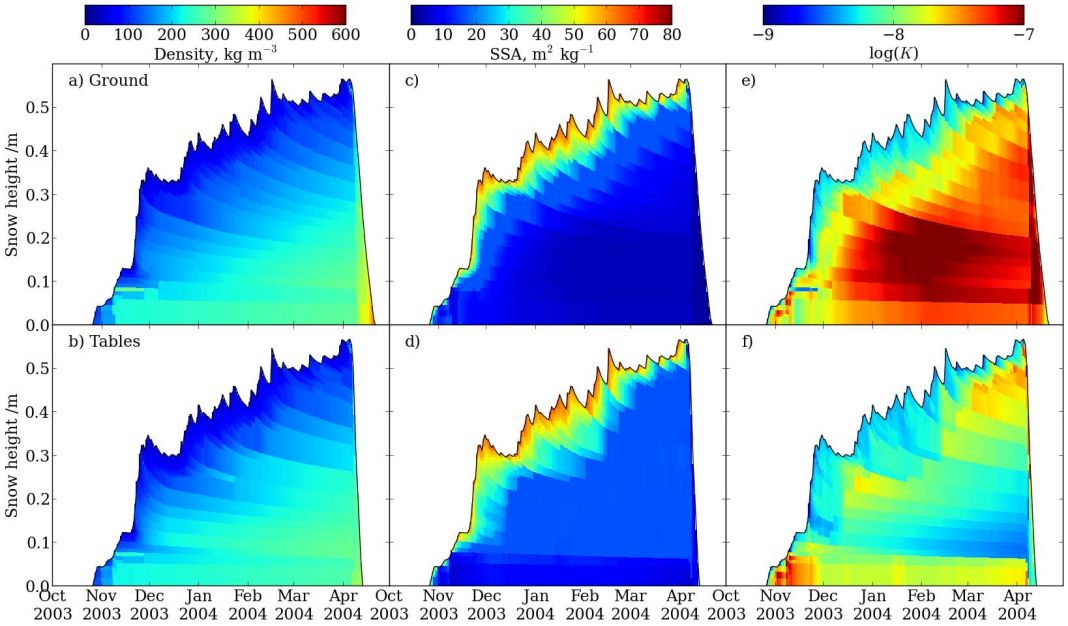

Fig. 8. Simulations of the vertical profiles of density, SSA and permeability on the ground and on tables using Crocus, over the whole season.

TCD
7, 2725–2759, 2013

Seasonal evolution of snow permeability under ET and TG conditions

F. Domine et al.

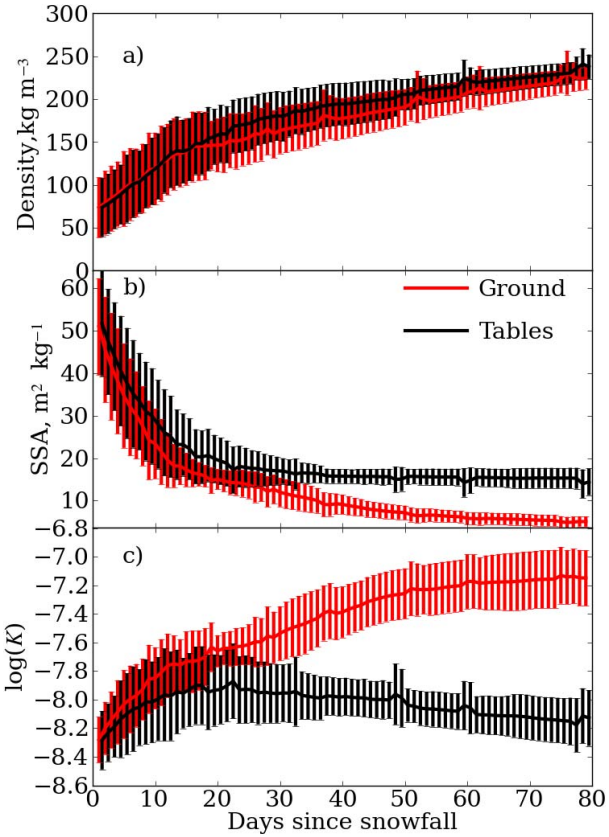

Fig. 9. Time evolution of the physical properties of all the snow layers making up the snowpack (density, SSA and permeability). All the layers, tracked by Crocus, were averaged. The standard deviation is shown. The different evolution on tables and ground shows clearly.

TCD
7, 2725–2759, 2013

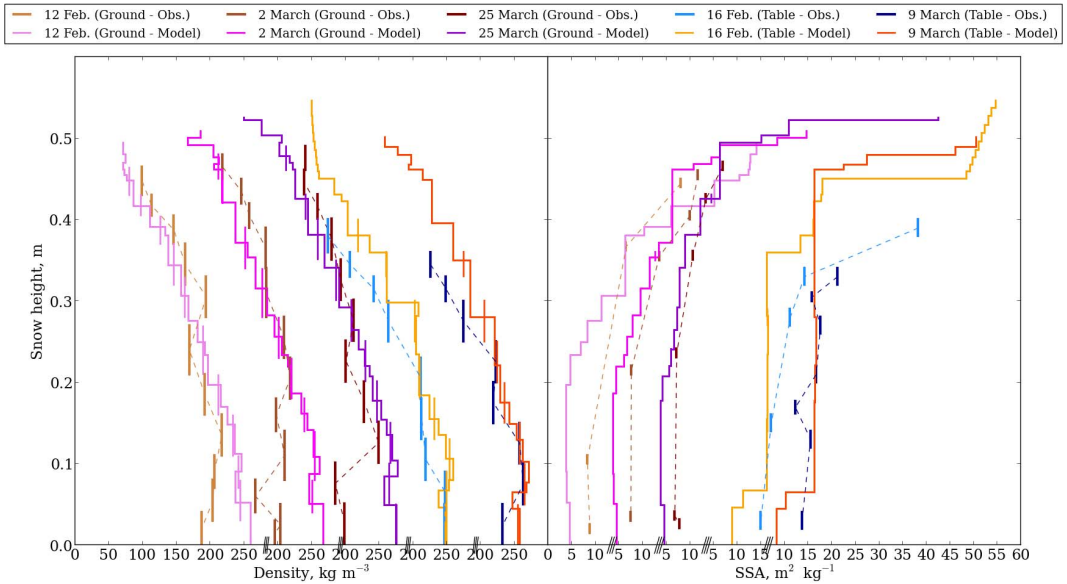

Fig. 10. Comparison of modeled and measured snow density (left) and SSA (right) for the ground and table snowpacks. Data are shown for the five profiles measured. For simulated densities, data are shown with high vertical resolution, and also with the resolution of the measurements, to facilitate comparison.

TCD
7, 2725–2759, 2013

Seasonal evolution of snow permeability under ET and TG conditions

F. Domine et al.

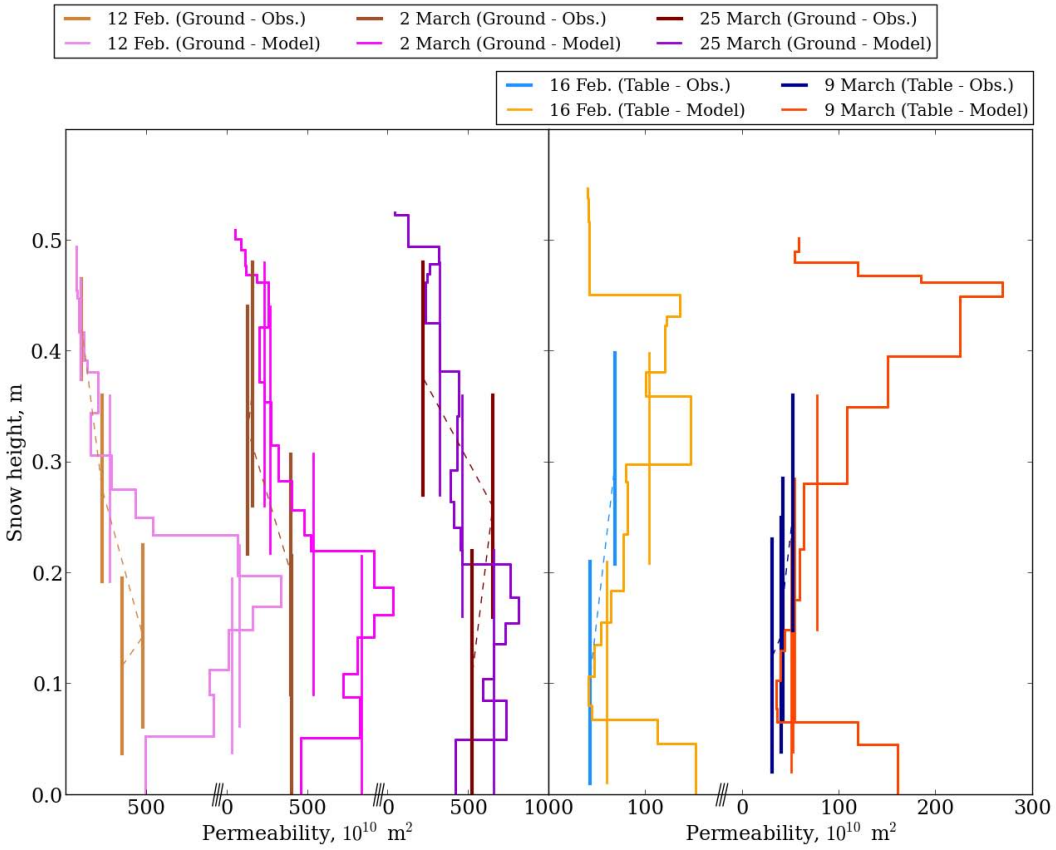

Fig. 11. Same as Fig. 10 for the permeability. Eq. (5) was used to obtain the simulated data at the resolution of the measurements.

TCD
7, 2725–2759, 2013

Seasonal evolution of snow permeability under ET and TG conditions

F. Domine et al.